

## Charge Transport and Quantum Interference Effects in Oxazole-Terminated Conjugated Oligomers

Songsong Li, Hao Yu, Kenneth Schwieter, Kejia Chen, Bo  
Li, Yun Liu, Jeffrey S. Moore, and Charles M. Schroeder

*J. Am. Chem. Soc.*, **Just Accepted Manuscript** • DOI: 10.1021/jacs.9b08427 • Publication Date (Web): 13 Sep 2019

Downloaded from [pubs.acs.org](https://pubs.acs.org) on September 13, 2019

### Just Accepted

“Just Accepted” manuscripts have been peer-reviewed and accepted for publication. They are posted online prior to technical editing, formatting for publication and author proofing. The American Chemical Society provides “Just Accepted” as a service to the research community to expedite the dissemination of scientific material as soon as possible after acceptance. “Just Accepted” manuscripts appear in full in PDF format accompanied by an HTML abstract. “Just Accepted” manuscripts have been fully peer reviewed, but should not be considered the official version of record. They are citable by the Digital Object Identifier (DOI®). “Just Accepted” is an optional service offered to authors. Therefore, the “Just Accepted” Web site may not include all articles that will be published in the journal. After a manuscript is technically edited and formatted, it will be removed from the “Just Accepted” Web site and published as an ASAP article. Note that technical editing may introduce minor changes to the manuscript text and/or graphics which could affect content, and all legal disclaimers and ethical guidelines that apply to the journal pertain. ACS cannot be held responsible for errors or consequences arising from the use of information contained in these “Just Accepted” manuscripts.

# Charge Transport and Quantum Interference Effects in Oxazole-Terminated Conjugated Oligomers

*Songsong Li<sup>1,4†</sup>, Hao Yu<sup>2†</sup>, Kenneth Schwieter<sup>3</sup>, Kejia Chen<sup>2</sup>, Bo Li<sup>2</sup>, Yun Liu<sup>4</sup>,  
Jeffrey S. Moore<sup>1,3,4</sup>, and Charles M. Schroeder<sup>1,2,3,4\*</sup>*

<sup>1</sup>Department of Materials Science and Engineering, University of Illinois at Urbana-Champaign, Urbana, Illinois, 61801, United States

<sup>2</sup>Department of Chemical and Biomolecular Engineering, University of Illinois at Urbana-Champaign, Urbana, Illinois, 61801, United States

<sup>3</sup>Department of Chemistry, University of Illinois at Urbana-Champaign, Urbana, Illinois, 61801, United States

<sup>4</sup>Beckman Institute for Advanced Science and Technology, University of Illinois at Urbana-Champaign, Urbana, Illinois, 61801, United States

†Contributed equally to this work.

\*To whom correspondence should be addressed. Email: [cms@illinois.edu](mailto:cms@illinois.edu)

**Keywords:** single molecule conductance, oxazole, molecular electronics, quantum interference, scanning tunneling microscope break-junction (STM-BJ)

**Abstract**

Charge transport in single molecule junctions critically depends on the chemical identity of anchor groups used to connect molecular wires to electrodes. In this work, we report the charge transport properties of conjugated oligomers with oxazole anchors, focusing on the role of the heteroatom substitution position in terminal oxazole groups. Our results show that oxazole serves as an efficient anchor group to form stable gold-molecule-gold junctions. We further observe quantum interference (QI) effects in oxazole-terminated phenylene molecular junctions, including destructive QI in meta-substituted phenyl rings and constructive QI in para-substituted phenyl rings containing terminal oxazole groups with the same chemical constitution on both termini (i.e. O<sub>5</sub>O<sub>5</sub> (5-oxazolyl) or O<sub>4</sub>O<sub>4</sub> (4-oxazolyl) linkages on both termini). Surprisingly, meta-substituted phenyl rings with non-equivalent constitutions (i.e. O<sub>4</sub>O<sub>5</sub> oxazole terminal linkages) show unexpectedly higher conductance compared to para-substituted analogs. These results suggest that charge transport in oxazole-terminated molecules is determined by the heteroatom substitution position of the oxazole anchor in addition to the aryl substitution pattern of the pi-conjugated core. Our results further show that conjugated molecules with homogeneous oxazole linkages obey a quantum circuit rule such that  $G_{O4-p-O4}/G_{O4-m-O4} = G_{O5-p-O5}/G_{O5-m-O5}$ , where  $G$  is molecular conductance. Overall, our work provides key insight into the development of new chemistries for molecular circuitry in the rapidly advancing field of single molecule electronics.

## INTRODUCTION

Recent advances in single molecule electronics have uncovered new chemistries and molecular systems that offer new fundamental insight into molecular electronic structure and charge transport.<sup>1-6</sup> Single molecule junctions generally contain a central bridge terminated by anchor groups that are used to connect molecular wires to electrodes.<sup>7</sup> Charge transport in molecular junctions significantly depends on the chemical identity of the anchor groups and on the nature of the chemical interactions at the electrode-molecule interface.<sup>8</sup> From this view, anchor groups are conveniently divided into two categories based binding interactions with metal electrodes: dative anchors bind to metal electrodes via coordination interactions, whereas covalent anchors provide direct metal-molecule contacts.<sup>7</sup> Prior work has explored a wide array of anchor groups for single molecule junctions, including dative anchors with  $\pi$ -donor groups such as fullerene,<sup>9</sup> dative anchors with lone pair donors such as primary amine (-NH<sub>2</sub>),<sup>10</sup> pyridine<sup>11,12</sup>, cyano (-CN),<sup>13</sup> isocyano (-NC),<sup>14</sup> isothiocyanate (-NCS),<sup>15</sup> selenol (-Se),<sup>16</sup> methyl thio (-SCH<sub>3</sub>),<sup>17</sup> phosphine,<sup>18</sup> nitro (-NO<sub>2</sub>),<sup>19</sup> and carboxylic acid (-COOH),<sup>20</sup> and covalent anchors such as thiol (-SH),<sup>20</sup> trimethyltin,<sup>21</sup> trimethylsilyl-terminated alkynes,<sup>22</sup> and diazonium.<sup>23</sup>

Chemical anchors are a critical component of single molecule junctions and often play a key role in determining molecular conductance in these systems. In particular, the chemical identity of dative linker groups often determines whether charge transport occurs by a highest occupied molecular orbital (HOMO)-dominated or lowest unoccupied molecular orbital (LUMO)-dominated pathway.<sup>7</sup> In addition, chemical anchors have been used to tune symmetric or

1  
2  
3  
4 asymmetric coupling interactions between molecular wires and electrode surfaces. In one case,  
5  
6 molecular design was used to install dative and covalent anchor groups at two termini of a junction,  
7  
8  
9 thereby generating a molecular rectifier.<sup>24</sup>  
10

11  
12 Quantum interference (QI) effects play an essential role in the charge transport properties of  
13  
14 molecular electronics.<sup>25,26</sup> Single molecule conductance measurements have shown that meta-  
15  
16 substituted phenyl groups generally exhibit lower conductance than para-substituted phenyls.<sup>27</sup> In  
17  
18 a meta-substituted phenyl ring, the de Broglie electron waves emerge out-of-phase after traversing  
19  
20 different molecular conduction pathways, thereby resulting in destructive QI. On the other hand,  
21  
22 para-substituted phenyl rings give rise to constructive QI and consequently higher levels of  
23  
24 conductance compared to the meta-substituted analog.<sup>25</sup> QI effects also arise in anchor groups with  
25  
26 conjugated rings, though only a few chemical anchors for molecule-metal junctions feature a fused  
27  
28 ring structure. Anchor groups containing a conjugated ring structure have several potential  
29  
30 molecular conduction pathways, complicating the molecular design of quantum circuits due to  
31  
32 quantum effects.<sup>28</sup> Despite recent progress, the effect of heteroatom substitution position on QI  
33  
34 effects is not fully understood in the context of anchor groups with conjugated ring structures.  
35  
36  
37  
38  
39  
40  
41  
42  
43

44 In this work, we show that oxazole serves an efficient anchor group to form stable gold-  
45  
46 molecule-gold junctions, resulting in conductive molecular wires. We systematically explore the  
47  
48 role of heteroatom substitution position on QI in oxazole-terminated molecular junctions using the  
49  
50 scanning tunneling microscope break-junction (STM-BJ) technique and density functional theory  
51  
52 (DFT) simulations. Our results show that oligophenyls terminated with oxazole exhibit an  
53  
54  
55  
56  
57  
58  
59  
60

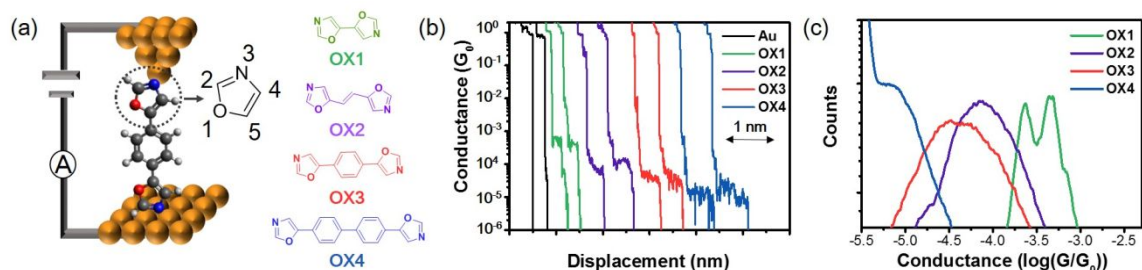


**Figure 1.** Charge transport in oxazole-terminated molecular wires. (a) Schematic of metal-molecule-metal junction and structures of compounds **OX1-OX4**. (b) Characteristic single molecule conductance traces for **OX1-OX4** molecular junctions. (c) Conductance histograms for **OX1-OX4**, with each constructed from >10,000 traces.

exponential conductance decay constant ( $\beta = 0.40 \text{ \AA}^{-1}$ ), comparable to amine-terminated analogs ( $\beta = 0.42 \text{ \AA}^{-1}$ ). Combined results from single molecule experiments and molecular modeling show that the nitrogen atom in the oxazole ring is the point-of-contact to the metal surface through the lone electron pair, similar to pyridine-based anchor groups.<sup>11</sup> Our results further reveal unexpected QI phenomena in oxazole-terminated molecular junctions. For oxazole-terminated molecules with the same chemical constitution on both termini, including  $O_5O_5$  (5-oxazolyl) or  $O_4O_4$  (4-oxazolyl) linkages, destructive QI is observed in meta-substituted phenyl molecular junctions. Surprisingly, our results show that meta-substituted phenyl rings with non-equivalent constitutions ( $O_4O_5$  oxazole linkages) exhibit constructive QI. Taken together, these results suggest that the heteroatom position in oxazole rings plays a key role in conductance, in addition to the arene substitution pattern in conjugated phenyl bridges. This work expands the library of chemical anchor groups and explores the effect of anchors with conjugated ring structures on QI, thereby opening new opportunities for molecular electronics.<sup>29</sup>

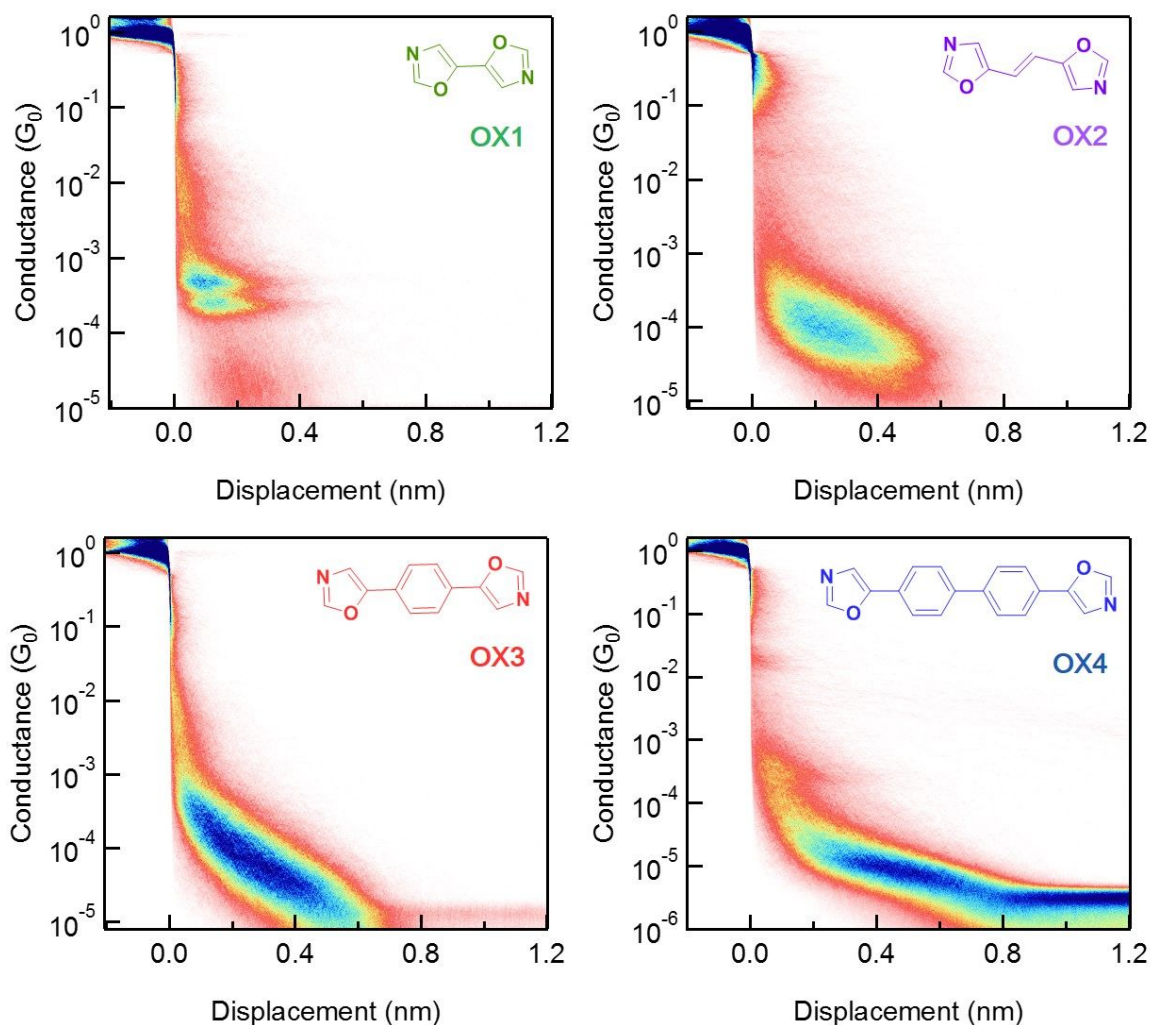


**Figure 2:** Two-dimensional (2D) conductance histograms for **OX1-OX4**, determined over a large ensemble of >10,000 individual molecules.

## RESULTS AND DISCUSSION

A series of oxazole-containing molecules was synthesized by van Leusen oxazole synthesis<sup>30</sup> and characterized by  $^1\text{H}$  and  $^{13}\text{C}$  NMR spectroscopies and mass spectrometry (Supporting Information, **Figures S1-S21**). We began by synthesizing oxazole-terminated oligomers with homogenous linkages at both termini with respect to heteroatom position on the oxazole ring. In particular, we synthesized 5,5'-bioxazole (**OX1**), (E)-1,2-bis(oxazol-5-yl)ethene (**OX2**), 1,4-

1  
2  
3  
4 bis(oxazol-5-yl)benzene (**OX3**), and 4,4'-bis(oxazol-5-yl)-1,1'-biphenyl (**OX4**), all of which  
5  
6 contain homogeneous linkages to oxazole anchors at the 5-position on the oxazole ring (**Figure**  
7  
8 **1a**). We further synthesized an expanded library of oxazole-terminated phenyl compounds with  
9  
10 varying arene substitution patterns (meta or para-linked) and defined linkages to the conjugated  
11  
12 ring oxazole anchors (**Table 1**). Additional details on the synthesis and chemical characterization  
13  
14 for all compounds can be found in the Supporting Information (**Figures S1-S21**).  
15  
16  
17  
18  
19

20 Single molecule conductance measurements were performed using a custom-built scanning  
21  
22 tunneling microscope break-junction (STM-BJ) technique under constant applied bias (250 mV)  
23  
24 in a liquid solvent (1,2,4-trichlorobenzene) (**Figure 1a**), as previously described.<sup>31-33</sup> In brief, the  
25  
26 STM-BJ experiment is performed by measuring molecular conductance at a constant applied bias  
27  
28 while pulling a gold tip away from a gold electrode surface, eventually leading to a break in the  
29  
30 molecular junction. **Figure 1b** shows characteristic single molecule conductance traces of **OX1-**  
31  
32 **OX4**, together with a break junction measurement in the absence of organic molecules (denoted  
33  
34 as Au). Plateaus in molecular conductance  $G$  at values less than the quantum unit of conductance  
35  
36 ( $G_0 = 2e^2/h = 77.5 \mu\text{S}$ ) correspond to charge transport through organic molecules bridging the  
37  
38 junction between the gold electrodes. Single molecule pulling experiments are generally repeated  
39  
40 for thousands of trials to enable robust statistical analysis. In this way, one-dimensional (1D)  
41  
42 conductance histograms are generated over a large ensemble of approximately  $10^4$  molecules for  
43  
44 **OX1-OX4** (**Figure 1c**). Interestingly, we observe two peaks in the conductance histograms for  
45  
46 **OX1** but only a single peak for **OX2**, **OX3**, and **OX4**. We conjecture that the two distinct  
47  
48  
49  
50  
51  
52  
53  
54  
55  
56  
57  
58  
59  
60

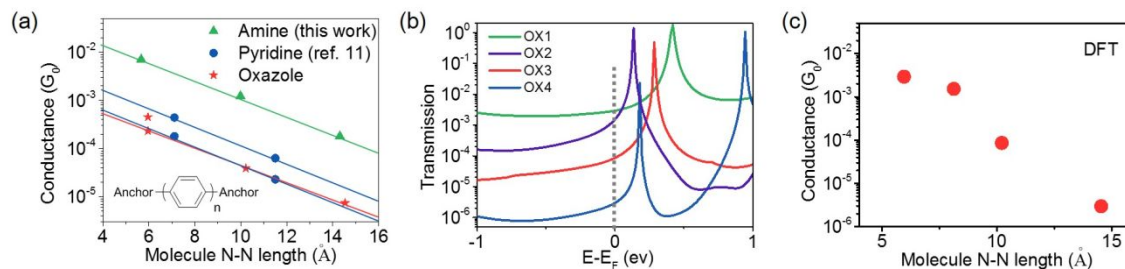


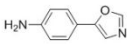
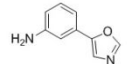
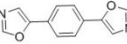
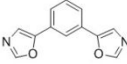
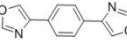
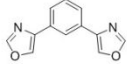
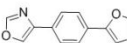
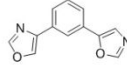
**Figure 3.** Charge transport behavior of oxazole-terminated oligomers determined by single molecule experiments and density functional theory (DFT) simulations. (a) Conductance peak values for amine-terminated (green,  $n = 1, 2, 3$ ), pyridine-terminated (blue,  $n = 0, 1$ ), and oxazole-terminated oligophenyls (red,  $n = 0, 1, 2$ ) plotted on a semi-log scale as a function of distance between N-N atoms on terminal anchors. Lines show fits to experimental data following a quantum tunneling model  $G=G_0e^{-\beta L}$ . (b) Transmission spectra of **OX1-OX4** determined by DFT simulations. (c) Calculated conductance values for **OX1-OX4** determined from DFT simulations.

conductance states in **OX1** are due to two binding geometries.<sup>12</sup> On the other hand, **OX2**, **OX3**, and **OX4**, adopt a single favored binding geometry, thereby resulting in distinct conductance peaks in the 1D histograms.

Two-dimensional (2D) conductance histograms of **OX1-OX4** are shown in **Figure 2**. 2D histograms show that average displacements during molecular pulling experiments tend to increase with increasing molecular length, such that **OX4** junctions can be stretched to approximately 0.8 nm. At an applied bias of 0.25 V, we found that the signal of **OX4** merged with the amplifier background noise. Therefore, we repeated the experiments and collected 2D conductance histograms of **OX4** at high bias (1 V) and observed a clear separation between signal and background (**Figure S22**). Average molecular conductance values for **OX1**, **OX3**, and **OX4** were determined from the peak values in the corresponding 1D histogram data and plotted on a semi-log scale versus the distance between nitrogen atoms in terminal anchor groups for each respective

1  
2  
3  
4 molecule (**Figure 3a**). In all cases, N-N distance was determined by density functional theory  
5  
6 (DFT) and corresponds to the distance between nitrogen atoms in terminal amines for amine-  
7  
8 terminated oligophenyls or N-N heteroatom distance between terminal oxazole rings. Our results  
9  
10 show that the average molecular conductance follows an exponential decay as a function of  
11  
12 molecular length, which suggests that charge transport follows a quantum tunneling model such  
13  
14 that  $\ln(G/G_0) = -\beta L$ , where  $\beta$  is the molecular decay constant  $\beta$  and  $L$  is the molecular length  
15  
16 between terminal nitrogen atoms. Using this approach, we determine a molecular decay constant  
17  
18  $\beta = 0.40 \pm 0.01 \text{ \AA}^{-1}$  for oxazole-terminated oligophenyls, which is consistent with amine-  
19  
20 terminated ( $\beta = 0.42 \pm 0.01 \text{ \AA}^{-1}$ ) (**Figure S23**) and pyridine-terminated oligophenyls ( $\beta = 0.5 \text{ \AA}^{-1}$ ).<sup>11,31</sup> These results suggest that oxazole anchors form robust molecular contacts with metallic  
21  
22 gold electrodes and enable stable measurements of conductance. To identify the specific anchoring  
23  
24 site linking oxazole rings to gold electrodes, we synthesized a control molecule 1,4-di(furan-2-  
25  
26 yl)benzene (**FU1**) for single molecule conductance experiments (**Figure S24**). In contrast to  
27  
28 oxazole-terminated **OX3**, no conductance signal was observed for furan-terminated compound  
29  
30 **FU1**, which confirms that the nitrogen heteroatom serves as the anchoring site in oxazole rings.  
31  
32  
33  
34  
35  
36  
37  
38  
39  
40  
41  
42

43 To further understand the charge transport properties of oxazole-terminated molecules, we  
44  
45 performed molecular modeling using nonequilibrium Green's function-density functional theory  
46  
47 (NEGF-DFT) via the Atomistix Toolkit package.<sup>34</sup> Molecular geometries for **OX1-OX4** are  
48  
49 optimized using DFT calculations performed on Spartan'16 Parallel Suite using the B3LYP  
50  
51 functional with a 6-31G (d,p) basis set. Following determination of geometry-optimized structures,  
52  
53  
54  
55  
56  
57  
58  
59  
60

Molecule name	Structure	Log( $G/G_0$ )	DFT Log( $G/G_0$ )	$G_{para}/G_{meta}$	DFT $G_{para}/G_{meta}$
A-p-O <sub>5</sub>		-3.24	-2.78	5.5	4.6
A-m-O <sub>5</sub>		-3.98	-3.44		
O <sub>5</sub> -p-O <sub>5</sub>		-4.41	-4.07	6.2	7.1
O <sub>5</sub> -m-O <sub>5</sub>		-5.20	-4.92		
O <sub>4</sub> -p-O <sub>4</sub>		-3.48	-3.65	6.6	6.0
O <sub>4</sub> -m-O <sub>4</sub>		-4.30	-4.43		
O <sub>4</sub> -p-O <sub>5</sub>		-4.77	-4.33	0.46	0.42
O <sub>4</sub> -m-O <sub>5</sub>		-4.43	-3.95		

**Table 1.** Molecular conductance properties of oxazole-terminated phenyls, including average conductance (expressed as  $\log(G/G_0)$ ) and  $G_{para}/G_{meta}$  from STM-BJ experiments and DFT simulations. Molecule names refer to amine anchors (A), oxazole anchors linked at the 5-oxazolyl (O<sub>5</sub>) or 4-oxazolyl (O<sub>4</sub>) position, and arene substitution pattern (p,m).

transmission functions are determined for relaxed molecules for **OX1-OX4** using NEGF-DFT (**Figure 3b**). For oxazole-terminated molecules **OX1-OX4**, the peaks in the transmission function appear between +0.1 to +0.5 eV, which corresponds to charge transport through the LUMO. We found that the slope of the transmission spectrum is positive at the Fermi level which suggests that the conduction orbital is in an unoccupied state, the thermopower becomes negative, and electrons are transported through the LUMO in **OX1-OX4**.<sup>35</sup> We also found that the magnitude of the transmission values for **OX1-OX4** close to Fermi energy are consistent with conductance trends in the experimental results (**Figure 3c**).

We next characterized the charge transport properties of a series of oxazole-terminated

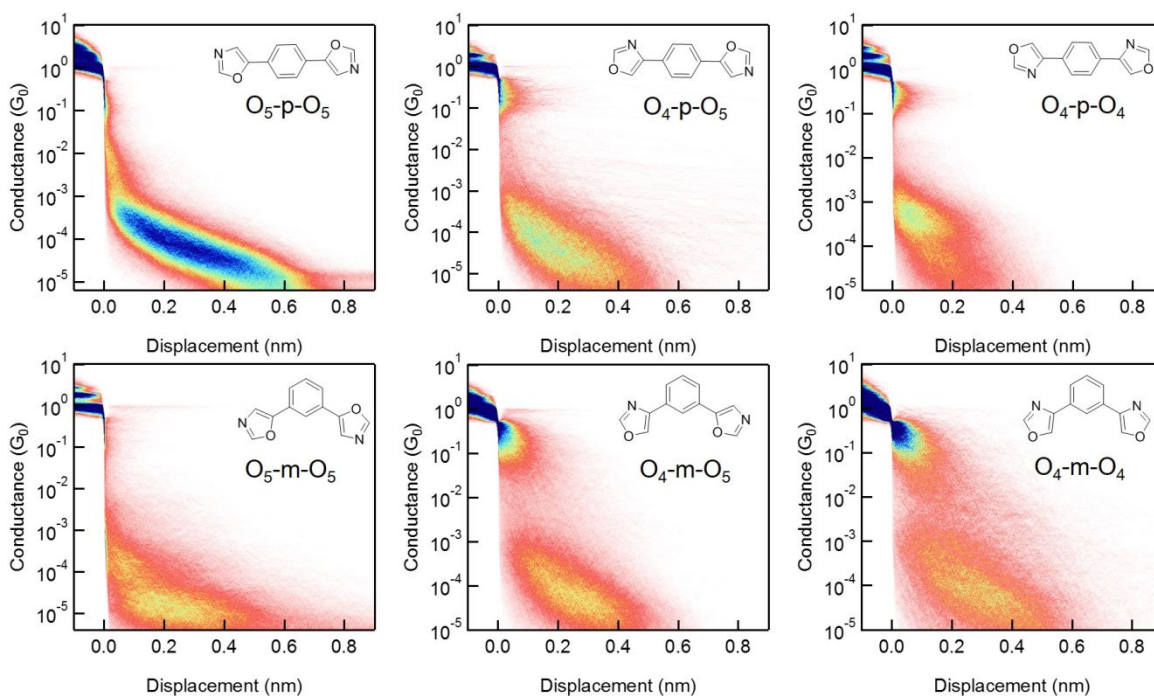


**Figure 4.** Two-dimensional (2D) molecular conductance histograms for a series of oxazole-terminated phenyl compounds at 0.25 V bias, each constructed from over 10,000 traces.

phenylene compounds with varying arene substitution patterns (para, meta) and different linkages to terminal oxazole groups (5-oxazolyl or 4-oxazolyl, denoted as  $O_5$  and  $O_4$ , respectively) (**Figure 4, Figures S25-S28 and Table 1**). To begin, we synthesized and studied the single molecule conductance of 1,4-bis(4-oxazolyl)benzene ( $O_4$ -**p**- $O_4$ ), 1,3-bis(4-oxazolyl)benzene ( $O_4$ -**m**- $O_4$ ), 1,4-bis(5-oxazolyl)benzene ( $O_5$ -**p**- $O_5$ , also denoted as **OX3**), and 1,3-bis(5-oxazolyl)benzene ( $O_5$ -**m**- $O_5$ ). Our results show that meta-substituted oxazole-terminated phenylenes with homogeneous  $O_5O_5$  and  $O_4O_4$  linkages show lower conductance than para-substituted analogs with homogeneous  $O_5O_5$  and  $O_4O_4$  linkages, consistent with a destructive quantum interference (QI) effect analogously observed in amine-linked,<sup>36</sup> methyl sulfide-linked,<sup>28</sup> and thiophene-linked<sup>27</sup> molecular junctions. Experimental results and NEGF-DFT simulation data in **Table 1** clearly show

1  
2  
3  
4 that the QI ratio of meta/para-linkage satisfies a quantum circuit rule such that  $G_{O_4-p-O_4}/G_{O_4-m-O_4} =$   
5  
6  $G_{O_5-p-O_5}/G_{O_5-m-O_5} \approx 6$ .<sup>37,38</sup> As a comparison, pyridine-terminated molecules also follow a quantum  
7  
8 circuit rule such that  $G_{ppp}/G_{pmp} = G_{mpm}/G_{mmm}$ , where the contribution to the conductance from the  
9  
10 central phenylene ring is independent of the anchor groups with para or meta-linkages.<sup>27</sup> From this  
11  
12 view, oxazole anchors offer an interesting opportunity to probe QI effects due to the asymmetric  
13  
14 nature of the five-membered ring associated with terminal oxazole groups. For oxazole-terminated  
15  
16 junctions with equivalent constitutions on both termini, we found that the conductance of  
17  
18 molecules with O<sub>4</sub>O<sub>4</sub> linkages is higher compared to their counterparts with O<sub>5</sub>O<sub>5</sub> linkages based  
19  
20 on most-probable conductance results and NEGF-DFT simulations, which further supports the  
21  
22 quantum circuit rule  $G_{O_4-p-O_4}/G_{O_5-p-O_5} = G_{O_4-m-O_4}/G_{O_5-m-O_5}$ .  
23  
24  
25  
26  
27  
28  
29

30 To further examine QI effects through oxazole-terminated molecular junctions with non-  
31  
32 equivalent constitutions on both termini, we synthesized and studied the molecular conductance  
33  
34 of 5-(4-(oxazol-4-yl)phenyl)oxazole (**O<sub>4</sub>-p-O<sub>5</sub>**) and 5-(3-(oxazol-4-yl)phenyl)oxazole (**O<sub>4</sub>-m-O<sub>5</sub>**).  
35  
36 From most-probable conductance results and NEGF-DFT simulations, our results show that the  
37  
38 conductance of **O<sub>4</sub>-p-O<sub>5</sub>** is lower than **O<sub>4</sub>-m-O<sub>5</sub>**, such that  $G_{O_4-p-O_5}/G_{O_4-m-O_5} < 0.5$ . Surprisingly,  
39  
40 these results suggest that the meta-substituted phenylene exhibits a higher conductance than the  
41  
42 para-substitute phenylene in oxazole-terminated molecules with heterogeneous O<sub>4</sub>O<sub>5</sub> linkages.  
43  
44 Recently, Li et al.<sup>39</sup> and Huang et al.<sup>40</sup> used electrochemical gating to tune QI, which revealed that  
45  
46 meta-substituted phenyl groups show higher conductance than para-substitute phenyls. On the  
47  
48 other hand, our results show that a meta-substituted phenylene group can exhibit a higher  
49  
50 molecular conductance relative to the para-substituted analog without external electrochemical  
51  
52  
53  
54  
55  
56  
57

gating<sup>41</sup>. In prior work, Borges et al. reported that meta-coupled bipyridine molecules show higher conductance through a  $\sigma$ -bonded system compared to the para-coupled analog.<sup>42</sup> For **O<sub>4</sub>-m-O<sub>5</sub>**, the electronic coupling occurs across seven bonds, whereas for **O<sub>4</sub>-p-O<sub>5</sub>** the coupling is through eight bonds. Therefore, we posit that **O<sub>4</sub>-m-O<sub>5</sub>** has a higher  $\sigma$  contribution to charge transport which gives rise to a larger total transmission for **O<sub>4</sub>-m-O<sub>5</sub>** compared to **O<sub>4</sub>-p-O<sub>5</sub>**. Similar observations were reported by Gorczak and coworkers,<sup>43</sup> who showed that meta-substitute biphenyl bridges exhibit a higher hole transfer rate compared to para-substitute analogs. Interestingly, this phenomenon was attributed to the asymmetric donor and acceptor states which leads to asymmetry in the molecular orbitals. In our work, we studied the molecular conductance of phenylenes containing heterogenous anchor groups based on oxazole-terminated O<sub>4</sub>O<sub>5</sub> linkages. For such heterogeneous linked molecules, we conjecture that one anchor group contributes constructive QI and the second anchor results in destructive QI. When coupled with a meta-substituted phenylene bridge with destructive QI, heterogeneous oxazole O<sub>4</sub>O<sub>5</sub> linkages can alter the overall QI in the molecular junction, thereby giving rise to unexpectedly high conductance in the meta-linked molecular bridge.

## CONCLUSION

In this work, we study the charge transport properties of a series of oxazole-terminated phenylene compounds with varying arene substitution patterns (para, meta) and different linkages to terminal oxazole rings using a combination of single molecule experiments and molecular models. Our results show that oxazole serves as a stable chemical anchor group for facilitating molecular

1  
2  
3  
4 connections to gold metal electrode surfaces. Oxazole-terminated ( $O_5$  linkage) oligophenyls  
5  
6 exhibit a decay constant  $\beta = 0.40 \pm 0.01 \text{ \AA}^{-1}$ , which is comparable with amine-terminated and  
7  
8 pyridine-terminated equivalents. In addition, we systematically studied QI phenomena through the  
9  
10 central phenyl ring and terminal oxazole ring. In particular, for oxazole-terminated junctions with  
11  
12 equivalent constitutions on both termini, which include  $O_4O_4$  and  $O_5O_5$  oxazole-terminated  
13  
14 molecules, the QI of the central phenylene follows a quantum circuit rule that  $G_{O_4-p-O_4}/G_{O_4-m-O_4} =$   
15  
16  $G_{O_5-p-O_5}/G_{O_5-m-O_5}$ . For oxazole-terminated junctions with non-equivalent constitutions on both  
17  
18 termini, including  $O_4O_5$  oxazole-terminated molecules, meta-substituted phenylene exhibits a  
19  
20 higher conductance compared to para-substitute phenylene. These results reveal the role of the  
21  
22 anchor group in controlling QI which facilitates an increased understanding of molecular  
23  
24 conductance in junctions with complex heterogeneous structures. Moving forward, this work could  
25  
26 aid in the design and development of new chemistries for molecular electronics.  
27  
28  
29  
30  
31  
32  
33  
34

### 35 36 **Associated Content**

### 37 38 **Supporting Information**

39  
40  
41 The Supporting Information is available free of charge on the ACS Publications website at DOI:  
42  
43 XXX. Description of chemical synthesis, chemical and physical characterization of oxazole-  
44  
45 terminated molecules, experimental details on STM-BJ, simulation methods, supporting text,  
46  
47 supporting figures.  
48  
49  
50  
51

### 52 53 **Corresponding Author**

54 [cms@illinois.edu](mailto:cms@illinois.edu)  
55  
56  
57

**ORCID**

Songsong Li: [0000-0001-9784-2877](https://orcid.org/0000-0001-9784-2877)

Hao Yu: [0000-0002-1594-769X](https://orcid.org/0000-0002-1594-769X)

Yun Liu: [0000-0001-7077-363X](https://orcid.org/0000-0001-7077-363X)

Charles M. Schroeder: [0000-0001-6023-2274](https://orcid.org/0000-0001-6023-2274)

**Notes**

The authors declare no competing financial interests.

**Acknowledgements**

We thank Prof. Latha Venkataraman and Dr. Yaping Zang for generously providing advice in building the STM-BJ instrument. This work was supported by the U.S. Department of Defense by a MURI (Multi-University Research Initiative) through the Army Research Office (ARO) through Award W911NF-16-1-0372 to C.M.S. and J.S.M.

**References**

- (1) Aviram, A.; Ratner, M. A. Molecular rectifiers. *Chemical Physics Letters* **1974**, *29*, 277.
- (2) Xu, B.; Tao, N. J. Measurement of single-molecule resistance by repeated formation of molecular junctions. *Science* **2003**, *301*, 1221.
- (3) Metzger, R. M. Unimolecular electronics. *Chemical Reviews* **2015**, *115*, 5056.
- (4) Aradhya, S. V.; Venkataraman, L. Single-molecule junctions beyond electronic transport. *Nature Nanotechnology* **2013**, *8*, 399.
- (5) Leary, E.; La Rosa, A.; González, M. T.; Rubio-Bollinger, G.; Agraït, N.; Martín, N. Incorporating single molecules into electrical circuits. The role of the chemical anchoring group. *Chemical Society Reviews* **2015**, *44*, 920.
- (6) Zang, Y.; Ray, S.; Fung, E. D.; Borges, A.; Garner, M. H.; Steigerwald, M. L.; Solomon,

1  
2  
3  
4 G. C.; Patil, S.; Venkataraman, L. Resonant Transport in Single Diketopyrrolopyrrole Junctions.  
5  
6 *Journal of the American Chemical Society* **2018**, *140*, 13167.

7  
8 (7) Su, T. A.; Neupane, M.; Steigerwald, M. L.; Venkataraman, L.; Nuckolls, C. Chemical  
9  
10 principles of single-molecule electronics. *Nature Reviews Materials* **2016**, *1*, 16002.

11  
12 (8) Leary, E.; La Rosa, A.; Gonzalez, M. T.; Rubio-Bollinger, G.; Agrait, N.; Martin, N.  
13  
14 Incorporating single molecules into electrical circuits. The role of the chemical anchoring group.  
15  
16 *Chemical Society Reviews* **2015**, *44*, 920.

17  
18 (9) Martin, C. A.; Ding, D.; Sørensen, J. K.; Bjørnholm, T.; van Ruitenbeek, J. M.; van der  
19  
20 Zant, H. S. Fullerene-based anchoring groups for molecular electronics. *Journal of the American*  
21  
22 *Chemical Society* **2008**, *130*, 13198.

23  
24 (10) Venkataraman, L.; Klare, J. E.; Tam, I. W.; Nuckolls, C.; Hybertsen, M. S.; Steigerwald,  
25  
26 M. L. Single-molecule circuits with well-defined molecular conductance. *Nano Letters* **2006**, *6*,  
27  
28 458.

29  
30 (11) Kamenetska, M.; Quek, S. Y.; Whalley, A.; Steigerwald, M.; Choi, H.; Louie, S. G.;  
31  
32 Nuckolls, C.; Hybertsen, M.; Neaton, J.; Venkataraman, L. Conductance and geometry of  
33  
34 pyridine-linked single-molecule junctions. *Journal of the American Chemical Society* **2010**, *132*,  
35  
36 6817.

37  
38 (12) Kim, T.; Darancet, P.; Widawsky, J. R.; Kotiuga, M.; Quek, S. Y.; Neaton, J. B.;  
39  
40 Venkataraman, L. Determination of Energy Level Alignment and Coupling Strength in 4,4' -  
41  
42 Bipyridine Single-Molecule Junctions. *Nano Letters* **2014**, *14*, 794.

43  
44 (13) Mishchenko, A.; Zotti, L. A.; Vonlanthen, D.; Bürkle, M.; Pauly, F.; Cuevas, J. C.; Mayor,  
45  
46 M.; Wandlowski, T. Single-Molecule Junctions Based on Nitrile-Terminated Biphenyls: A  
47  
48 Promising New Anchoring Group. *Journal of the American Chemical Society* **2011**, *133*, 184.

49  
50 (14) Kim; Beebe, J. M.; Jun, Y.; Zhu, X. Y.; Frisbie, C. D. Correlation between HOMO  
51  
52 Alignment and Contact Resistance in Molecular Junctions: Aromatic Thiols versus Aromatic  
53  
54

1  
2  
3  
4 Isocyanides. *Journal of the American Chemical Society* **2006**, *128*, 4970.

5  
6 (15)Ko, C.-H.; Huang, M.-J.; Fu, M.-D.; Chen, C.-h. Superior Contact for Single-Molecule  
7  
8 Conductance: Electronic Coupling of Thiolate and Isothiocyanate on Pt, Pd, and Au. *Journal of*  
9  
10 *the American Chemical Society* **2010**, *132*, 756.

11  
12 (16)Yasuda, S.; Yoshida, S.; Sasaki, J.; Okutsu, Y.; Nakamura, T.; Taninaka, A.; Takeuchi,  
13  
14 O.; Shigekawa, H. Bond fluctuation of S/Se anchoring observed in single-molecule conductance  
15  
16 measurements using the point contact method with scanning tunneling microscopy. *Journal of the*  
17  
18 *American Chemical Society* **2006**, *128*, 7746.

19  
20 (17)Garner, M. H.; Li, H.; Chen, Y.; Su, T. A.; Shangguan, Z.; Paley, D. W.; Liu, T.; Ng, F.;  
21  
22 Li, H.; Xiao, S. Comprehensive suppression of single-molecule conductance using destructive  $\sigma$ -  
23  
24 interference. *Nature* **2018**, *1*.

25  
26 (18)Kamenetska, M.; Koentopp, M.; Whalley, A.; Park, Y.; Steigerwald, M.; Nuckolls, C.;  
27  
28 Hybertsen, M.; Venkataraman, L. Formation and evolution of single-molecule junctions. *Physical*  
29  
30 *Review Letters* **2009**, *102*, 126803.

31  
32 (19)Zotti, L. A.; Kirchner, T.; Cuevas, J. C.; Pauly, F.; Huhn, T.; Scheer, E.; Erbe, A.  
33  
34 Revealing the role of anchoring groups in the electrical conduction through single-molecule  
35  
36 junctions. *Small* **2010**, *6*, 1529.

37  
38 (20)Chen, F.; Li, X.; Hihath, J.; Huang, Z.; Tao, N. Effect of anchoring groups on single-  
39  
40 molecule conductance: comparative study of thiol-, amine-, and carboxylic-acid-terminated  
41  
42 molecules. *Journal of the American Chemical Society* **2006**, *128*, 15874.

43  
44 (21)Batra, A.; Kladnik, G.; Gorjizadeh, N.; Meisner, J.; Steigerwald, M.; Nuckolls, C.; Quek,  
45  
46 S. Y.; Cvetko, D.; Morgante, A.; Venkataraman, L. Trimethyltin-mediated covalent gold-carbon  
47  
48 bond formation. *Journal of the American Chemical Society* **2014**, *136*, 12556.

49  
50 (22)Hong, W.; Li, H.; Liu, S.-X.; Fu, Y.; Li, J.; Kaliginedi, V.; Decurtins, S.; Wandlowski, T.  
51  
52 Trimethylsilyl-terminated oligo (phenylene ethynylene) s: an approach to single-molecule  
53  
54

1  
2  
3  
4 junctions with covalent Au–C  $\sigma$ -bonds. *Journal of the American Chemical Society* **2012**, *134*,  
5  
6 19425.

7  
8 (23)Hines, T.; Díez-Pérez, I.; Nakamura, H.; Shimazaki, T.; Asai, Y.; Tao, N. Controlling  
9  
10 Formation of Single-Molecule Junctions by Electrochemical Reduction of Diazonium Terminal  
11  
12 Groups. *Journal of the American Chemical Society* **2013**, *135*, 3319.

13  
14 (24)Batra, A.; Darancet, P.; Chen, Q. S.; Meisner, J. S.; Widawsky, J. R.; Neaton, J. B.;  
15  
16 Nuckolls, C.; Venkataraman, L. Tuning Rectification in Single-Molecular Diodes. *Nano Lett* **2013**,  
17  
18 *13*, 6233.

19  
20 (25)Lambert, C. Basic concepts of quantum interference and electron transport in single-  
21  
22 molecule electronics. *Chemical Society reviews* **2015**, *44*, 875.

23  
24 (26)Manrique, D. Z.; Huang, C.; Baghernejad, M.; Zhao, X.; Al-Owaedi, O. A.; Sadeghi, H.;  
25  
26 Kaliginedi, V.; Hong, W.; Gulcur, M.; Wandlowski, T. A quantum circuit rule for interference  
27  
28 effects in single-molecule electrical junctions. *Nature communications* **2015**, *6*, 6389.

29  
30 (27)Arroyo, C. R.; Tarkuc, S.; Frisenda, R.; Seldenthuis, J. S.; Woerde, C. H.; Eelkema, R.;  
31  
32 Grozema, F. C.; van der Zant, H. S. Signatures of quantum interference effects on charge transport  
33  
34 through a single benzene ring. *Angewandte Chemie* **2013**, *125*, 3234.

35  
36 (28)Aradhya, S. V.; Meisner, J. S.; Krikorian, M.; Ahn, S.; Parameswaran, R.; Steigerwald,  
37  
38 M. L.; Nuckolls, C.; Venkataraman, L. Dissecting contact mechanics from quantum interference  
39  
40 in single-molecule junctions of stilbene derivatives. *Nano letters* **2012**, *12*, 1643.

41  
42 (29)Xiang, D.; Wang, X.; Jia, C.; Lee, T.; Guo, X. Molecular-Scale Electronics: From  
43  
44 Concept to Function. *Chemical Reviews* **2016**, *116*, 4318.

45  
46 (30)Van Leusen, A.; Hoogenboom, B.; Siderius, H. A novel and efficient synthesis of  
47  
48 oxazoles from tosylmethylisocyanide and carbonyl compounds. *Tetrahedron Letters* **1972**, *13*,  
49  
50 2369.  
51  
52  
53  
54  
55  
56  
57  
58  
59  
60

1  
2  
3  
4 (31) Venkataraman, L.; Klare, J. E.; Nuckolls, C.; Hybertsen, M. S.; Steigerwald, M. L.  
5  
6 Dependence of single-molecule junction conductance on molecular conformation. *Nature* **2006**,  
7  
8 *442*, 904.

9  
10 (32) Zang, Y.; Ray, S.; Fung, E.-D.; Borges, A.; Garner, M. H.; Steigerwald, M. L.; Solomon,  
11  
12 G. C.; Patil, S.; Venkataraman, L. Resonant Transport in Single-Diketopyrrolopyrrole Junctions.  
13  
14 *Journal of the American Chemical Society* **2018**.

15  
16 (33) Li, B.; Yu, H.; Montoto, E.; Liu, Y.; Li, S.; Schwieter, K.; Rodríguez-López, J.; Moore,  
17  
18 J. S.; Schroeder, C. M. Intrachain Charge Transport through Conjugated Donor-Acceptor  
19  
20 Oligomers. *ACS Applied Electronic Materials* **2019**, *1*, 7.

21  
22 (34) Cai, Z.; Lo, W.-Y.; Zheng, T.; Li, L.; Zhang, N.; Hu, Y.; Yu, L. Exceptional single-  
23  
24 molecule transport properties of ladder-type heteroacene molecular wires. *Journal of the American*  
25  
26 *Chemical Society* **2016**, *138*, 10630.

27  
28 (35) Komoto, Y.; Fujii, S.; Iwane, M.; Kiguchi, M. Single-molecule junctions for molecular  
29  
30 electronics. *Journal of Materials Chemistry C* **2016**, *4*, 8842.

31  
32 (36) Kiguchi, M.; Nakamura, H.; Takahashi, Y.; Takahashi, T.; Ohto, T. Effect of anchoring  
33  
34 group position on formation and conductance of a single disubstituted benzene molecule bridging  
35  
36 Au electrodes: change of conductive molecular orbital and electron pathway. *The Journal of*  
37  
38 *Physical Chemistry C* **2010**, *114*, 22254.

39  
40 (37) Lambert, C. J.; Liu, S. X. A Magic Ratio Rule for Beginners: A Chemist's Guide to  
41  
42 Quantum Interference in Molecules. *Chemistry—A European Journal* **2018**, *24*, 4193.

43  
44 (38) Sangtarash, S.; Huang, C.; Sadeghi, H.; Sorohhov, G.; Hauser, J. r.; Wandlowski, T.;  
45  
46 Hong, W.; Decurtins, S.; Liu, S.-X.; Lambert, C. J. Searching the hearts of graphene-like  
47  
48 molecules for simplicity, sensitivity, and logic. *Journal of the American Chemical Society* **2015**,  
49  
50 *137*, 11425.

51  
52 (39) Li, Y.; Buerkle, M.; Li, G.; Rostamian, A.; Wang, H.; Wang, Z.; Bowler, D. R.; Miyazaki,  
53  
54

1  
2  
3  
4 T.; Xiang, L.; Asai, Y.; Zhou, G.; Tao, N. Gate controlling of quantum interference and direct  
5  
6 observation of anti-resonances in single molecule charge transport. *Nature Materials* **2019**, *18*,  
7  
8 357.  
9

10 (40)Huang, B.; Liu, X.; Yuan, Y.; Hong, Z.-W.; Zheng, J.-F.; Pei, L.-Q.; Shao, Y.; Li, J.-F.;  
11  
12 Zhou, X.-S.; Chen, J.-Z. Controlling and Observing Sharp-Valleyed Quantum Interference Effect  
13  
14 in Single Molecular Junctions. *Journal of the American Chemical Society* **2018**, *140*, 17685.  
15

16 (41)Li, X.; Tan, Z.; Huang, X.; Bai, J.; Liu, J.; Hong, W. Experimental investigation of  
17  
18 quantum interference in charge transport through molecular architectures. *Journal of Materials*  
19  
20 *Chemistry C* **2019**.  
21

22 (42)Borges, A.; Fung, E. D.; Ng, F.; Venkataraman, L.; Solomon, G. C. Probing the  
23  
24 Conductance of the  $\sigma$ -System of Bipyridine Using Destructive Interference. *The Journal of*  
25  
26 *Physical Chemistry Letters* **2016**, *7*, 4825.  
27

28 (43)Gorzak, N.; Renaud, N.; Tarkuç, S.; Houtepen, A. J.; Eelkema, R.; Siebbeles, L. D.;  
29  
30 Grozema, F. C. Charge transfer versus molecular conductance: molecular orbital symmetry turns  
31  
32 quantum interference rules upside down. *Chemical Science* **2015**, *6*, 4196.  
33  
34  
35  
36  
37  
38  
39  
40  
41  
42  
43  
44  
45  
46  
47  
48  
49  
50  
51  
52  
53  
54  
55  
56  
57  
58  
59  
60

## TOC Graphic



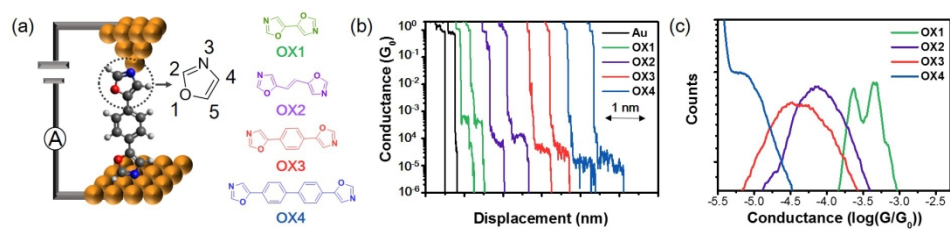


Figure 1

167x40mm (300 x 300 DPI)

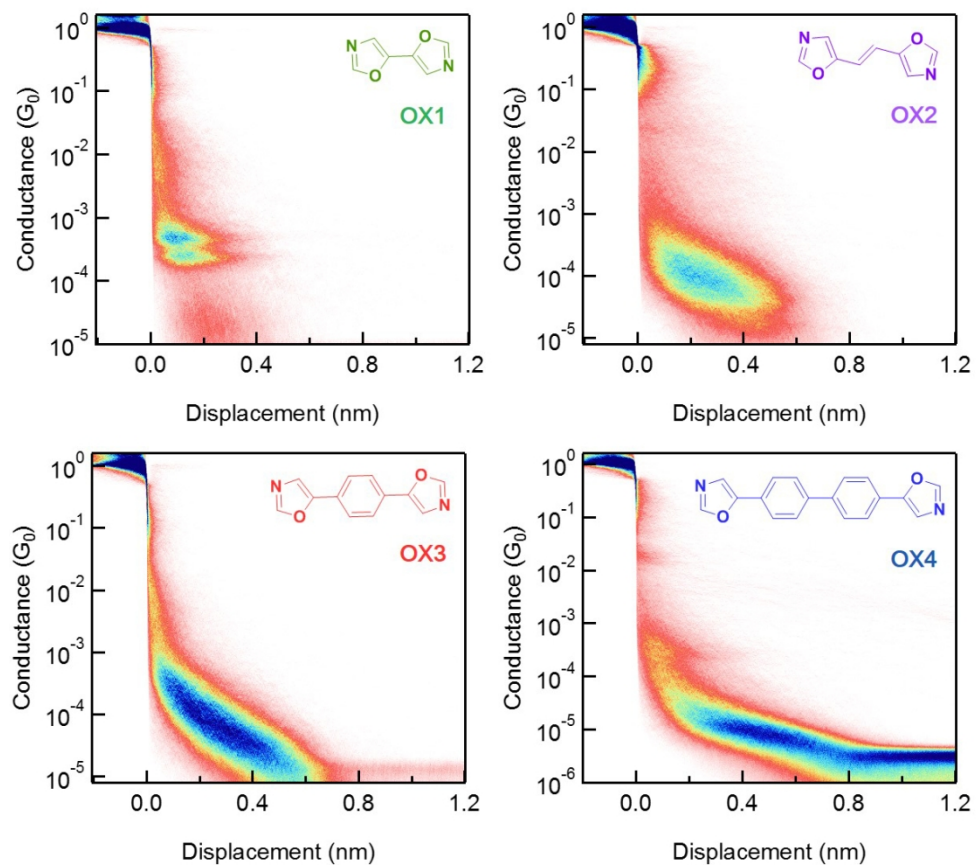


Figure 2

106x93mm (300 x 300 DPI)

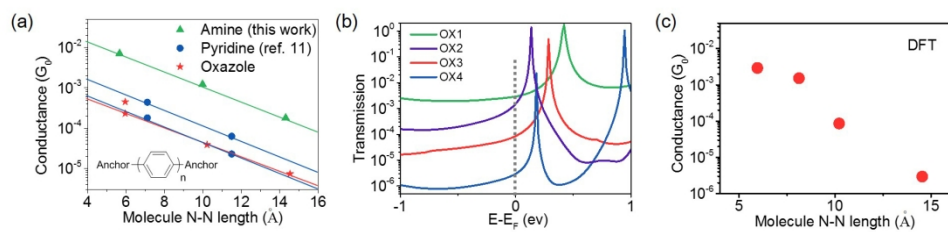


Figure 3

169x40mm (300 x 300 DPI)

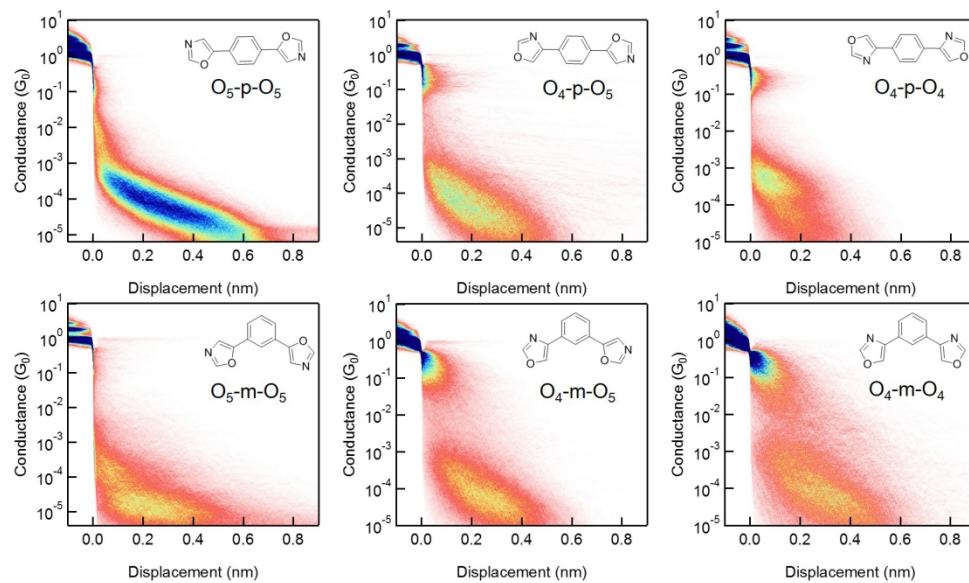


Figure 4

158x91mm (300 x 300 DPI)

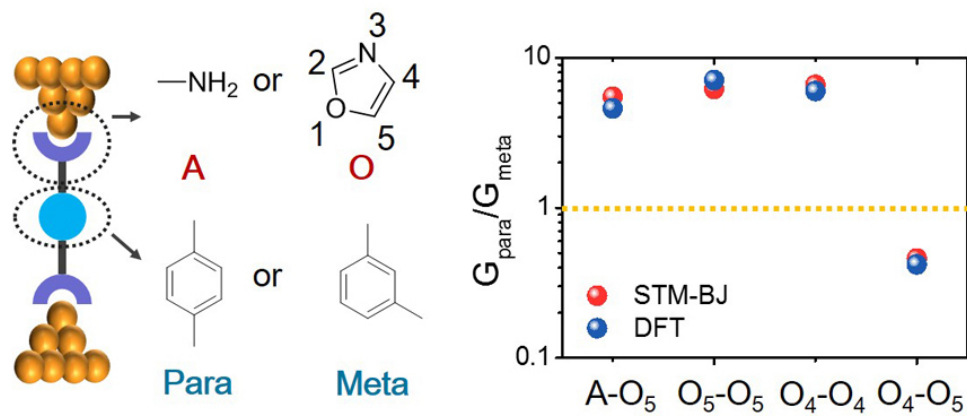


Table of contents graphic

75x33mm (300 x 300 DPI)